Prenatal exposure to ultrasound waves impacts neuronal migration in mice

Eugenius S. B. C. Ang, Jr.*†, Vicko Gluncic*†, Alvaro Duque*, Mark E. Schafer‡, and Pasko Rakic*§

*Department of Neurobiology and Kavli Institute for Neuroscience, Yale Medical School, Sterling Hall of Medicine, Room C-318, 333 Cedar Street, New Haven, CT 06510; and ‡Sonic Tech, Inc., 23 Brookline Court, Ambler, PA 19002

Communicated by Dale Purves, Duke University Medical Center, Durham, NC, June 29, 2006 (received for review August 5, 2005)

Neurons of the cerebral neocortex in mammals, including humans, are generated during fetal life in the proliferative zones and then migrate to their final destinations by following an inside-to-outside sequence. The present study examined the effect of ultrasound waves (USW) on neuronal position within the embryonic cerebral cortex in mice. We used a single BrdU injection to label neurons generated at embryonic day 16 and destined for the superficial cortical layers. Our analysis of over 335 animals reveals that, when exposed to USW for a total of 30 min or longer during the period of their migration, a small but statistically significant number of neurons fail to acquire their proper position and remain scattered within inappropriate cortical layers and/or in the subjacent white matter. The magnitude of dispersion of labeled neurons was variable but systematically increased with duration of exposure to USW. These results call for a further investigation in larger and slower-developing brains of non-human primates and continued scrutiny of unnecessarily long prenatal ultrasound exposure.

brain malformations | cerebral cortex | embryonic development

A fundamental feature of cerebral cortical organization is that positions of its neuronal constituents into horizontal (laminar) and vertical (radial) arrays ultimately define their connectivity and function (1). Cortical neurons acquire appropriate positions by migration from the site of their origin in the proliferative zones lining the cerebral ventricle, according to a precise schedule (2, 3) and along well defined pathways (4–6). When the rate of neuronal migration and the sequence of arrival are altered because of genetic and/or environmental factors, various consequences, including abnormal behavior, have been observed (7–13). In terms of orientation and directionality of movement, neuronal migration to the cerebral cortex can be classified into radial (proceeding radially from the ventricular to the pial surface) (5, 14) and tangential (running parallel to the brain surface) (15–17). Contact interaction between migrating neurons and the surfaces of neighboring cells plays a decisive role in selecting the migratory pathway and determining their final position (18, 19). Neuronal migration involves translocation of the nucleus and the surrounding cytoplasm with the leading process, which requires rearrangement of the cytoskeleton (20, 21). As a consequence of these complex cellular and molecular interactions, the process of neuronal migration is highly sensitive to a variety of biological, physical, and chemical agents, as well as to specific genetic mutations (7–13). For example, repeated exposure of the rodent and primate fetal brain to environmental agents, such as alcohol (9), drugs (22), neurotrophic viruses (23), and ionizing irradiation (24, 25), causes misplacement of neurons and behavioral deficits.

To our knowledge, the effect of ultrasound waves (USW) on the rate of migration in the cerebral cortex has never been tested, although it has been reported that the exposure of pregnant mice and non-human primates to USW may affect the behavior of their exposed offspring (26, 27). There also is some evidence that the frequent exposure of the human fetus to USW is associated with a decrease in newborn body weight (28, 29), an increase in the frequency of left-handedness (30), and delayed speech (31).

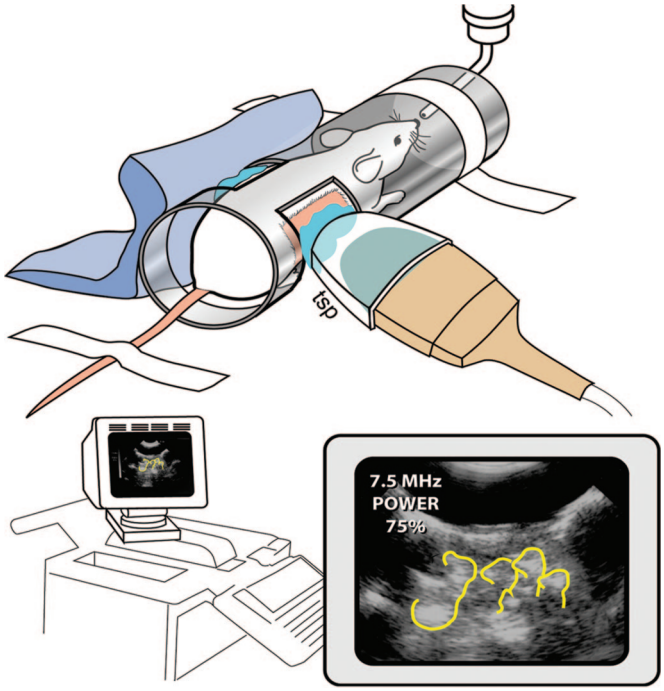

Fig. 1. The experimental design of the system used for exposure of pregnant mice to USW. The mouse is placed in the tube chamber with abdomen embedded in conductant jelly and separated from the transducer by a tissue stand-off pad (TSP). Diagnostic levels of USW were delivered during 5–45 min. The embryos were monitored on the screen, and pulse, oxygenation, and temperature in the mothers were recorded (35).

In addition, it was reported that diagnostic levels of ultrasound can disrupt membrane attachments or cells both *in vitro* (32, 33) and *in vivo* (34) and alter the cell cycle of the intestinal epithelium *in vivo* (35). Because ultrasound energy is a high-frequency mechanical vibration (36), we hypothesized that it might influence membrane-mediated, cell-to-cell attachments and/or nuclear translocation essential for neuronal migration. Because the migratory neurons and the adjacent radial glial guides in the embryonic brain are surrounded by extracellular spaces filled with low-viscosity fluids (5), the USW might affect cell motility through radiation force or microstreaming (36). In this study, we examined the possible effect of USW on neuronal migration in mice at a late stage of corticogenesis, when the

Conflict of interest statement: No conflicts declared.

Freely available online through the PNAS open access option.

Abbreviations: USW, ultrasound wave(s); E*n*, embryonic day *n*; P*n*, postnatal day *n*.

See Commentary on page 12661.

†E.S.B.C.A. and V.G. contributed equally to this work.

§To whom correspondence should be addressed. E-mail: pasko.rakic@yale.edu.

Table 1. Overview of experimental conditions and results

	Schedule				Control/USW-exposed					Effect		
Litter code	Duration, min	Period	$N \times$ min	Hr betw.	No. of pups	No. of columns	No. of counted cells	Mean dispersion	SD of dispersion	Dispersion difference, %	t	P
C1/U1	420	8	12 × 35	4	7/7	42/42	3,669/3,722	0.133/0.190	0.019/0.019	5.68	$t(12) = 5.602$	0.000
Total					7/7	42/42	3,669/3,722					
C2/U2	210	8	7 × 30	6	7/8	42/48	2,676/3,664	0.049/0.093	0.022/0.047	4.39	$t(26) = 3.177$	0.004
C3/U3	210	8	7 × 30	6	7/6	42/36	2,747/2,559					
Total					14/14	84/84	5,429/6,223					
C4/U4	60	12	2 × 30	12	6/6	36/36	3,918/4,084	0.050/0.113	0.023/0.067	6.38	$t(59) = 5.072$	0.000
C5/U5	60	12	2 × 30	12	14/11	84/66	6,021/5,174					
C6/U6	60	12	2 × 30	12	12/12	72/72	11,620/15,203					
Total					32/29	192/174	21,559/24,461					
C7/U7	30	12	2 × 15	12	11/14	66/84	9,284/12,547	0.059/0.089	0.031/0.047	3.05	$t(68) = 3.183$	0.002
C8/U8	30	12	2 × 15	12	14/10	84/60	11,531/7,562					
C9/U9	30	12	2 × 15	12	10/11	60/66	8,962/10,312					
Total					35/35	210/210	29,777/30,421					
C10/U10	15	12	1 × 15	N/A	12/12	72/72	8,239/8,113	0.047/0.052	0.021/0.021	0.47	$t(70) = 0.984$	0.346
C11/U11	15	12	1 × 15	N/A	11/14	66/84	9,696/11,702					
C12/U12	15	12	1 × 15	N/A	10/13	60/78	9,597/12,927					
Total					33/39	198/234	27,532/32,742					
C13/U13	5	12	1 × 5	N/A	10/13	60/78	8,273/9,084					
C14/U14	5	12	1 × 5	N/A	10/9	60/54	8,523/7,271	0.028/0.031	0.014/0.016	0.34	$t(40) = 0.742$	0.463
Total					20/22	120/132	16,796/16,355					
NC1	0	N/A	N/A	N/A	7	42	3,013	0.061	0.022	N/A	N/A	N/A
NC2	0	N/A	N/A	N/A	8	47	4,724					
NC3	0	N/A	N/A	N/A	15	89	9,645					
Total					30	178	17,382					
14/14 (grand total)					141/146	846/876	104,752/113,924	0.052/0.080	0.031/0.056	2.82%	$t(285) = 5.219$	0.000

Shown under the exposure schedule during the E16–E18 period (''Schedule'') is the period between BrdU injection and first exposure (''Period''), total exposure schedule shown as the number of exposures times the number of minutes per exposure (''$N \times$ min''), and the number of hours between exposures (''Hr betw.''). Across all durations, the mean number of stained cells was somewhat larger in the ultrasound condition (mean = 780.30, SD = 245.38, $N = 146$) than in the control condition (mean = 742.92, SD = 220.65, $N = 141$). However, that difference was not statistically significant [$t(285) = 1.355$, $P = 0.176$]. The power to detect a medium effect ($d = 0.5$) with this sample size is 0.99; the power to detect a small effect ($d = 0.2$) is 0.39. Dispersion is defined as the percentage of cells in bins 6–10. Dispersion difference is defined as the mean dispersion for controls minus the mean dispersion for USW-exposed animals. The means and standard errors of dispersion by duration and condition also are shown in Fig. 5*A*. Values for t test are from a two-tailed test with independent samples. The grand total does not include values for 0 duration (normal control) or the additional experiment using the different ultrasound system. Note that three sections were taken from each pup, and two columns were taken from each section. NA, not applicable; NC, normal control.

migratory pathways are the longest and, thus, may be most vulnerable.

Results

Qualitative Analysis. Pregnant mice were injected on embryonic day (E)16 with the DNA-replication marker BrdU to label dividing cells in the proliferative zone destined for superficial cortical layers 2 and 3 (37). Then, within the next 3 days, while these cells were migrating across the cerebral wall, the animals were exposed to multiple sessions of USW in a specially designed experimental system (Fig. 1). The total exposure to USW ranged from 5 to 420 min, delivered in multiple individual sessions (Table 1). The controls were subjected to identical procedures, except for exposure to USW. The pregnancies were brought to term (E19), and the pups were nursed by their mothers and then euthanized on postnatal day (P)10. The brains were fixed, sectioned in the coronal plane, and stained with propidium iodide to show cortical lamination, followed by immunocytochemical staining of the BrdU to expose the final positions of cells generated at E16 (Fig. 2 *C–H*). Double-labeling with neuron-specific marker NeuN (BrdU/NeuN) showed that the majority of cells (USW, 89.5 ± 0.6%; control, 88.4 ± 3.8%) generated at E16 in controls and USW-exposed animals are neurons, irrespective of their position (Fig. 3 *A–C*). The remaining 10–12% of BrdU-labeled cells are either neurons that were not labeled with NeuN or glial cells. In selected specimens, the BrdU cells were double-immunolabeled with markers for superficial-layer (Brn1) or deep-layer (FoxP2) neurons. To assess the pattern of migration and positioning of E16-born cortical neurons, the number of BrdU-labeled cells within a grid made up of 10 equally sized bins (Fig. 2 *E* and *H*) was imaged and counted by investigators blind to the experimental conditions, followed by statistical analysis.

Examination of the routine histological preparations did not reveal a difference in brain size and cytoarchitectonic organization between the control and USW-exposed animals (Fig. 2 *A–C* and *F*). In the counterstained sections from the controls, the majority of $BrdU^+$ cells accumulated, as expected, in bins 2/3, which roughly correspond to superficial cortical layers 2/3, whereas a small number of $BrdU^+$ cells were scattered in the lower bins (Fig. 2 *D* and *E*). In contrast, in many mice exposed to USW, $BrdU^+$ cells were more dispersed, as illustrated in the cortex of a P10 mouse exposed *in utero* to USW for a total of 60 min (Fig. 2 *G* and *H*). More specifically, layers 2/3 contained usually a smaller number of $BrdU^+$ cells, whereas the deeper layers and the underlying white matter contained more of such cells (Fig. 2 *G* and *H*). In some cases, ectopic $BrdU^+$ cells formed a distinct band near the lateral cerebral ventricle (Fig. 2*H*, white arrowheads) that resemble periventricular ectopias. When these ectopic $BrdU^+$ cells occurred, it was easy to distinguish the

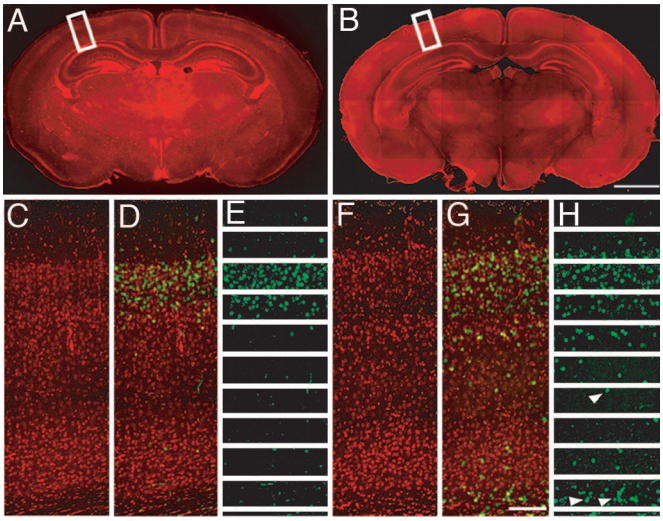

Fig. 2. Histological and immunohistochemical staining of sham and USW cortical slices. (*A* and *B*) Coronal sections across the cerebral wall in P10 control mouse (*A*) and mouse exposed to USW for 60 min between E17 and E18 (*B*). Quantification of BrdU-labeled cells was then performed (white boxes). (*C–E*) Control section from P10 controls animals. (*F–H*) Sections from P10 animals exposed as embryos to 60 min of USW. Neurons labeled with BrdU are stained green, and the slice was counterstained with propidium iodide, which is stained red. (*E* and *H*) The sections were divided into 10 equally spaced bins, with bin 1 starting at the pia and bin 10 ending near the ependymal surface. Notice the lower number of BrdU-labeled cells in the upper layers compared with the larger number in the deeper layers and subjacent white matter (white arrowheads). (Scale bars: *B*, 1.8 mm; *G*, 130 μm.)

exposed brains from the control brains, even upon visual inspection of the immunostained sections (Fig. 2, compare *E* with *H*). However, detailed quantitative analysis was needed to discern the change in pattern of cell dispersion in most cases and to expose the systematic difference between the two groups of animals.

Quantitative Analysis. The pattern of distribution for BrdU-labeled cells was highly variable; therefore, to quantify the degree of their deviation from the norm according to exposure time, BrdU-counterstained cells were plotted for controls and the mice were exposed to USW for various durations (Fig. 4 and Table 1). Examination of the brains of mice exposed multiple times for a total of 420 min (12 exposures, 35 min each exposure), 210 min (7 exposures, 30 min each exposure), 60 min (2 exposures, 30 min each exposure), and 30 min (2 exposures, 15 min each exposure) of USW, respectively, showed a consistent overall pattern of a smaller number of $BrdU^+$ cells situated in the upper cortical layers and a greater number in the lower layers and throughout the subcortical white matter, compared with control brains (Fig. 4 *A–D*). This difference in cell pattern was statistically significant (*t* test; see Table 1). In animals exposed to USW for 15 and 5 min, the effect was not statistically significant (Fig. 4 *E* and *F*). However, when the data were pooled together, across all durations, mice exposed prenatally to USW as a group contained a smaller percentage of $BrdU^+$ cells in the upper cortical layers (e.g., bin 2) and a larger percentage in the deeper layers as well as in the subcortical white matter (bins 4–10), compared with the controls (Fig. 4*G*). In addition, the majority of ectopic $BrdU^+$ cells located in layer VI and the subjacent white matter were double-labeled with NeuN (Fig. 3 *A–C*) and did not stain with lower cortical layer markers such as FoxP2 (Fig. 3 *D–F*). Furthermore, some of these ectopic $BrdU^+$ cells still retained upper-cortical-layer markers, such as Brn1 (Fig. 3 *G–I*), which suggests that these cells were neurons

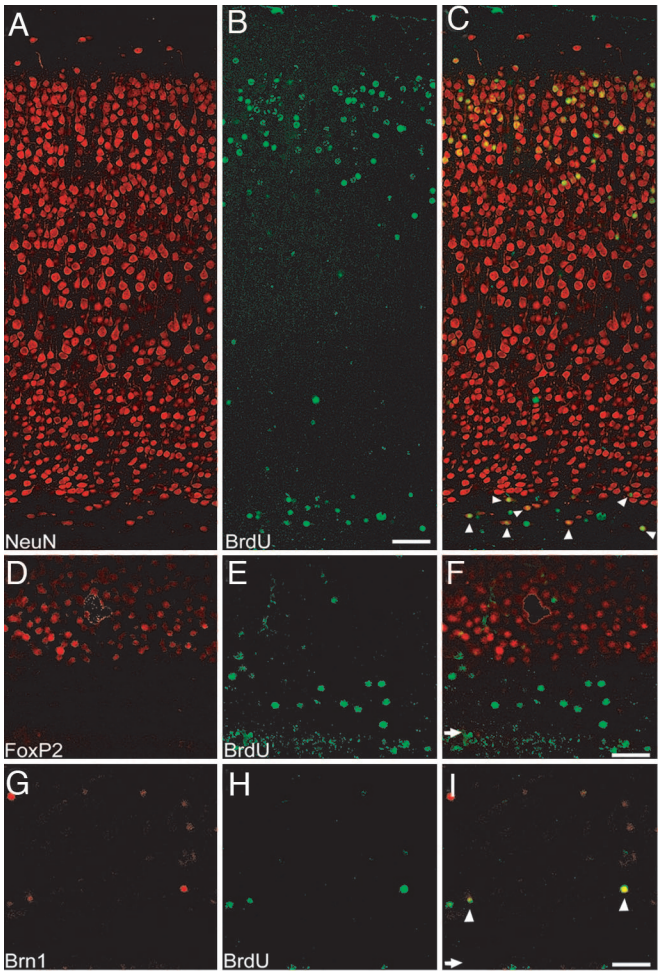

Fig. 3. Double-labeling of cortical slices exposed to USW for a cumulative dose of 30 min. (*A–C*) Staining for NeuN and BrdU and the merge of the two, respectively. The majority of $BrdU^+$ cells are $NeuN^+$, including those in layer 6 and subjacent white matter (white arrowheads in *C*). (*D–F*) No double-labeling for FoxP2, a marker for lower cortical layers, is present. Shown are $BrdU^+$ cells in layer 6 and subjacent white matter. (*G–I*) Some $BrdU^+$ cells in the subjacent white matter also label with Brn1, a marker of upper cortical layers (white arrowheads in *I*). (*F* and *I*) White arrows show the level of the ependyma in these images. (Scale bars: *C*, 72 μm; *F* and *I*, 65 μm.)

destined to superficial layers that were arrested along their migratory pathway and not located in their proper position.

Detailed examination of the effect of USW exposure at each duration and across all durations showed that the best individual-level measure of cell dispersion was the proportion of $BrdU^+$ cells found in the lower half of each brain section within bins 6–10 (Fig. 5 *A* and *B*). Multiple linear regression analyses of over 218,000 $BrdU^+$ cells obtained from 1,722 scans of 287 brains (146 exposed and 141 control) indicate that USW have an effect on final neuronal positioning in the mouse cerebral cortex ($P < 0.0001$) (Fig. 5 *A* and *B*). For example, under the experimental conditions used, doubling exposure time from 15 min to 30 min increased the number of cells in the lower layers from 5% to 9%. Increasing exposure to 60 min increased dispersion to 11%, which was a statistically significant level ($P > 0.0001$). At 210 min, the mean increase of 9% did not fit the expected response curve but was in the expected direction. However, at a total of 420 min exposure, we observed the largest dispersion of 19%. Although the results at shorter durations are relatively small, we do not know whether a 4% increase in dispersion of cells, as seen

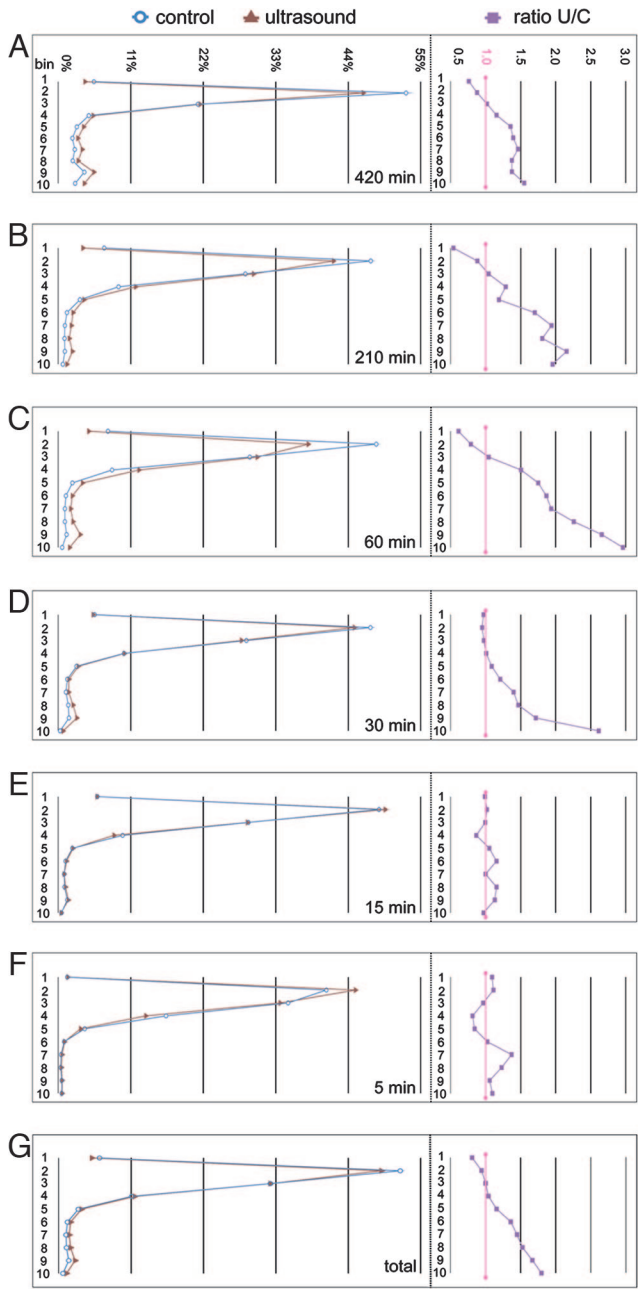

Fig. 4. Percentage of cells in each bin averaged across all animals in each exposure duration, shown by condition. (*A Left–F Left*) Line graphs showing the percent of cells in each bin for experimental and control animals for exposure durations of 420, 210, 60, 30, 15, and 5 min, respectively. For durations >15 min, the proportion of cells in the lower five bins was significantly higher for exposed than for control animals. (*A Right–F Right*) Line graphs showing the ratio of the percentage of cells in ultrasound-exposed versus control animals (U/C) for each bin. For durations >15 min, the small differences in the absolute magnitudes in the lower bins represent large proportional increases. (*G*) (*Left*) The average percentage of cells in each bin for all 146 experimental animals and 141 sham controls across all durations. Note the excess of cells in the lower bins for the exposed animal. (*Right*) Line graph showing the ratio of the percentage of cells in ultrasound versus control animals for each bin. The small difference in the absolute magnitudes in the lower bins represents large proportional increases.

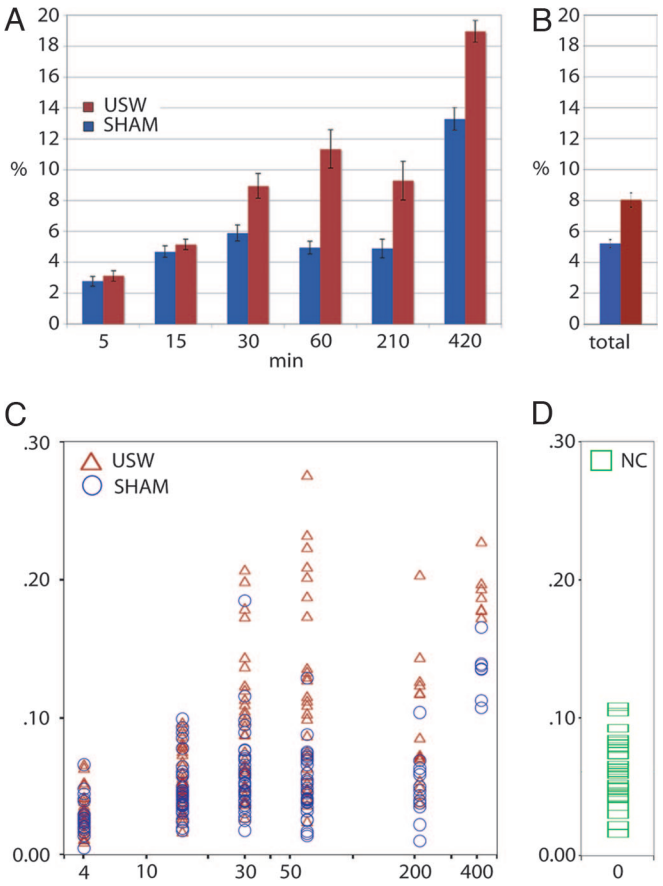

Fig. 5. Dispersion of BrdU$^+$ cells for USW and controls by duration of exposure. Dispersion is defined as the percentage of cells in bins 6–10. (*A*) The mean dispersion by condition and duration, with error bars showing the standard errors. (*B*) The mean dispersion for control and experimental animals across all durations with the Y-bars showing the standard errors. (*C*) A scatter plot by condition and duration for USW (red) and sham control (blue) conditions. Dispersion increases systematically with the length of exposure to USW. Dispersion also increases with sham exposure, although not as quickly as with ultrasound. (*D*) A scatter plot by condition with 0 min of duration for normal controls. The mean dispersion for the normal control condition was not significantly different from the 5-, 15-, 30-, 60-, and 210-min exposures. NC, normal control.

from the difference between 5- and 15-min exposures, is sufficient to compromise the normal cerebral cortical functions (Fig. 5*A*).

The cumulative dose–response curve using all seven experimental groups indicates that longer ultrasound exposure causes a larger effect (Fig. 5*C*), with a trend toward a smaller percentage of cells being in the upper cortical layers and a larger percentage in the lower layers and the white matter. Interestingly, there also is an increase in dispersion in the 420-min sham condition over normal controls (Fig. 5 *C* and *D*). This increase in cell dispersion may be due to the indirect effect of stress experienced by pregnant animals during prolonged exposure to the experimental procedure. Although the sample size at 420 min is small (two litters, seven sham pups and seven USW-exposed pups) (Table 1), the possibility of the role of stress in causing cell dispersion at long exposures during cortical development is worthy of a more detailed examination.

To further test the possibility that stress alone increases dispersion, we compared statistically all sham control conditions versus the normal control condition (Fig. 5 *C* and *D*). The normal control condition had a mean dispersion of 6.1% with an SD of 2.2% and an SE of 0.6% (n = 30) (Fig. 5*D* and Table 1). A post hoc comparison of all of the means using the Student–Newman–Keuls test indicated that the normal controls were not statistically different from the sham controls with 5, 15, 30, 60,

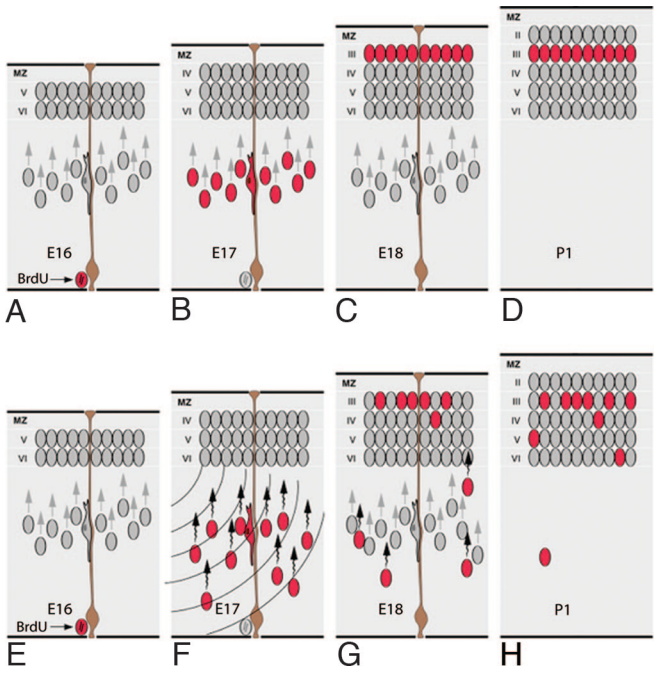

Fig. 6. Schematic representation of the progression of neuronal migration to the superficial cortical layers in the normal mouse. (*A–D*) Most cells labeled with BrdU at E16 arrive in the cortex by E18, and, by P1, those cells become surpassed by subsequently generated neurons. Eventually, these cells will settle predominantly in layers 2 and 3 of the cerebrum. (*E–H*) Model of the USW effect. When cells generated at E16 are exposed to USW, they slow down on E17, and some remain in the white matter or are stacked in the deeper cortical layers.

and 210 min of exposure but were different statistically from the 420-min exposure. This finding indicates that the stress due to the experimental procedure at durations of 210 min or below did not play a significant role in causing the cell dispersion seen in the sham conditions. At durations of 420 min, it is possible that the stress of this long exposure leads to increased cell dispersion above the normal control condition. However, it is difficult to completely assess durations of 420 min and above because some pups from USW-exposed mothers were either resorbed or cannibalized at birth (Table 1). In fact, no pups survived to P10 in pregnant mice exposed to 600 min of USW, although the sham control mouse gave birth to a full liter that survived until P10 (data not shown).

To confirm our results, we performed one more independent experiment with a more advanced and current ultrasound system (see *Material and Methods*) and a different operator. Four of nine pups from a litter exposed to USW for 60 min exhibited ectopic $BrdU^+$ cells forming near the lateral cerebral ventricle (Fig. 7*F*, which is published as supporting information on the PNAS web site), similar to that seen with the original ultrasound system (Fig. 2*H*). No pups were affected like this in any of the nine pups of the sham control litter (Fig. 7*C*). These types of periventricular ectopias also were not seen in normal control animals.

Discussion

This study shows that exposure of the embryonic mouse to USW can affect neuronal migration in the cerebral cortex and thereby prevent some neurons from attaining their final proper position. Because this effect is relatively small, it is not possible to predict the magnitude of dispersion in any single case. In fact, the control brains also contained a variable number of neurons scattered within the white matter, and we have even encountered exceptions in which individual brains from the control groups displayed a seemingly abnormal distribution of $BrdU^+$ cells. The variability encountered within the exposed group of animals indicates that there may be large individual differences in susceptibility. However, the linear arrangement of the embryos in the U-shaped mouse uterus precludes their equal exposure to USW and may contribute to the variability of the effects observed. Thus, USW has a predicable effect only when the large population of exposed animals is compared with unexposed controls by using multiple regression analysis and only at total exposure durations of 30 min or longer.

The cellular and molecular mechanisms of the effect of USW on migrating neurons observed in this study are unknown. At the frequencies and intensities we have used (see *Material and Methods*; see also *Supporting Text*, Tables 2–5, and Figs. 8–14 which are published as supporting information on the PNAS web site), it is unlilely that cavitation or temperature changes play a role in the effects noted (36). The dosimetry data and output parameters suggest that the mechanism may be a nonthermal, noncavitational, mechanically mediated effect, perhaps involving radiation force or microstreaming, or shear effects on cellular walls (38, 39). These mechanical effects could interfere with the delicate adhesion between the migratory neurons and the surface of migratory substrates, such as radial glial shafts, which serve as guides (5, 6, 14). The USW may also disturb exocytosis, essential for the extension of the leading tip of migrating neurons or disrupt cytoskeletal rearrangement essential for the translocation of the nucleus within its leading process (18, 20, 21, 37). Based on the present results, the effect on other forms of cell motility, such as tangential neuronal migration (13, 15, 17) or spinning of the mitotic spindle (40), cannot be excluded. Finally, although we cannot fully estimate the contribution of the indirect, humorally mediated effect of stress caused by the exposure of pregnant mothers to the experimental procedure, it appears to play a role only in extended exposures (420 min) based on comparisons between normal control durations and all sham control durations.

One plausible model of the observed effect of USW on cellular events in the fetal cerebral wall is illustrated in Fig. 6. Normally, cells generated in the proliferative ventricular zone at E16 migrate radially during the next two days (E17 and E18) and settle to the prospective layer 2/3 to be bypassed by the subsequently generated, unlabeled neurons that settle mostly above them in the upper tiers of layer 2 (Fig. 6). We hypothesize that, if cells generated at E16 that were en route to the cortex were slowed by exposure to USW, some of them would not arrive on time at the most superficial position between the developing cortical plate and the marginal zone (Fig. 6*G*). As a result, these cells become intermixed with the earlier-generated neurons within the lower cortical layers or remain in the subjacent white matter (Fig. 6*H*). The ectopic cells would then develop abnormal synaptic connectivity resulting in behavioral deficits, as has been observed in the mutant mice with malposition of neurons (7). These ectopic cells can also cause abnormal electrical discharge associated with epilepsy (10).

Perhaps the most obvious question raised by these results is their possible relevance for cortical development in humans. The principal ultrasound beam characteristics (beam width, time-averaged intensity, and mechanical and thermal indices) used in this study were well within clinical norms for fetal exams. Although the frequency used in the present study was slightly above standard obstetrical clinical practice (6.7 MHz versus 3.5–5.0 MHz), the latest ultrasound equipment with three-dimensional reconstruction and tissue harmonic imaging often employs even higher frequencies. The pulse average intensity was slightly above Food and Drug Administration guidelines, but the exposimetry measurements were set up as worst-case (full water path) scenarios, and the levels measured at the location of the fetuses are not considered excessive. In addition, in our

exposures, the ultrasound parameters and total exposure time are comparable with or below those used by commercial medically nonindicated prenatal ultrasound videos.

There are, however, huge differences in the number of neurons and the size of the cerebral cortex between mouse and human (41). Thus, in spite of the use of tissue stand-off pad, the distance between the exposed cells and transducer in our experiments is shorter than in human. Furthermore, the duration of neuronal production and the migratory phase of cortical neurons in the human fetus lasts ≈18 times longer than in mice (between 6 and 24 weeks of gestation, with the peak occurring between 11 and 15 weeks), compared with the duration of only ≈1 week (between E11 and E18) in the mouse (2, 4, 16). Thus, an exposure of 30 min represents a much smaller proportion of the time dedicated to development of the cerebral cortex in human than in mouse and, thus, could have a lesser overall effect, making human corticogenesis less vulnerable to USW.

There are also some reasons to think that the USW may have a similar or even greater impact on neuronal migration in the human fetal brain. First, migrating neurons in the human forebrain are only slightly larger than in the mouse, and, with the acoustic absorption provided by the tissue stand-off pad, the amount of energy absorbed within a comparable small volume of tissue during the USW exposure was in the same general range (*Supporting Text*, Tables 2–5, and Figs. 8–14). Second, the migratory pathway in the convoluted human cerebrum is curvilinear and at least an order of magnitude longer (4). Thus, the number of neurons migrating along the same radial glial fascicle, particularly at the later stages of corticoneurogenesis, is much larger and their routes are more complex (42), increasing the chance of a cell going astray from its proper migratory course. Third, the inside-to-outside settling pattern of isochronously generated neurons in primates is more precise than in rodents (3, 6) and thus, the tolerance for malpositioning may be smaller. In addition, different functional areas in the primate cortex are generated by different schedules (43) so that exposure to USW may potentially affect selective cortical areas and different layers, depending on the time of exposure, potentially causing a variety of symptoms.

In conclusion, it is not known whether or to what extent USW affects migrating neurons in developing humans. Identifying the position of isochronously generated neurons requires the technique of labeling DNA replication, a procedure that cannot be used in humans; therefore, the misplaced solitary cells in the cortex due to migratory disturbance could be missed upon neuropathological examination. The problem of detection is exacerbated by the small number of ectopic cells and the need for quantitative analysis to detect them. However, it is important to emphasize that even a small number of ectopic cells might, as a result of specific position and inappropriate connectivity, be a source of epileptic discharge or abnormal behavior. Although we have not as yet generated behavioral data, previous studies in rodents and primates indicate that prenatal exposure to USW may affect higher brain function of the offspring (26, 27). Furthermore, there are numerous human neuropsychiatric disorders that are thought to be the result of misplacement of cells as a consequence of abnormal neuronal migration (e.g., 8, 10, 12, 22–24). Therefore, our results in pregnant mice support the recommendations by the Food and Drug Administration that warn against the use of medically nonindicated or commercial prenatal ultrasound videos (44). Our results also call for careful testing of the nonthermal effects of USW at the potentially vulnerable intense period of cortical neurogenesis in the human fetus (45). Furthermore, it is essential to examine the possible effects of USW on cortical development in non-human primates, where the duration of embryogenesis and the size and complexity of migratory pathways are more similar to those in humans.

Materials and Methods

Exposure Procedure. An unanesthetized pregnant mouse was held in position within an exposure chamber made from a cardboard tube; the lateral surfaces of the tube had been cut to allow exposure of the mouse's abdominal wall to the ultrasound transducer (Fig. 1). The posterior half of the mouse body was embedded in acoustic gel. A water bag was acoustically coupled to the side of the mouse opposite the transducer to minimize the possibility of standing waves or reflections that might affect the exposure. The mouse's abdomen was shaved to ensure proper acoustical coupling between the ultrasound transducer and the skin.

For ultrasound exposure, we used an Ultramark 4 Plus (ATL, Bothell, WA) ultrasound system and an Access 10 transducer (frequencies 5M, 7.5S, and 10S). We selected an ultrasound system that has been routinely used in human medical clinics (36), and we used a 2-cm-thick tissue stand-off pad over the abdomen of unanesthetized pregnant mice. Unanesthetized pregnant mice were exposed to B-mode, 6.7-MHz, pulsed USW with a pulse duration of 0.2 ms and a scanning rate of 11 frames per second for 5–35 min in different schedules, total duration, and pregnancy time points (Table 1). A 2-cm-thick stand-off pad was placed between the transducer face and the abdomen of the mouse. The stand-off pad positioned the fetuses in the nearer uterine horn at the probe's focal point (2.1 cm, with a focal range from 1.3 to 4.0 cm). Dosimetry testing of the ultrasound system showed spatial peak pulse average intensities (I_{sppa}) of 330 W/cm^2, and spatial peak time average intensity (I_{spta}) of 1.5 mW/cm^2 when measured in water. The estimated I_{sppa} at the fetal locations was on the order of 1 W/cm^2 (see *Quantification of Ultrasound Exposure* and *Supporting Text*, Table 2, and Figs. 9–14 for ultrasound output parameters for the system). For the single confirmatory experiment done by using a different ultrasound system, a M2540A ultrasound system (model M2540-67000; Phillips, Bothell, WA) was used with a 15-6L transducer.

In an independent group of anesthetized exposed and sham control animals, pulse and oxygenation were monitored during the procedures by using a Novametrix pulse oxymeter (model 513; Medical Systems, Wallingford, CT). The thermistor data logger LogR (Barnant Company, Barrington, IL) was used to assess rectal/core temperature in treated animals and sham controls. Our data showed that there was not a statistically significant change in either pulse rate or core temperature in animals exposed to ultrasound.

Quantification of Ultrasound Exposure. The ultrasonic output parameters of the ATL UltraMark 4 Plus system were measured according to published international standards (46, 47) and the current measurement guidelines of the U.S. Food and Drug Administration (48) and by using the appropriate calibrated measurement equipment (Acoustic Measurement System measurement tank and software and Bilaminar Membrane Hydrophone model S5 with preamplifier; Sonora Medical Systems, Longmont, CO) (49). Measurements were conducted without the ultrasonic stand-off pad, which resulted in a worst-case exposure condition. Table 2, which is published as supporting information on the PNAS web site, summarizes the relevant output parameters at 2.5 cm from the transducer face, which would correspond to the depth of the fetuses when using a stand-off pad. The results are shown for the values directly measured in a water tank ("In water") and estimates of tissue exposure parameters ("Attenuated") according to the methodology of the Food and Drug Administration (44). For comparison, also listed in Table 2 are the current regulatory limits for medical diagnostic ultrasound equipment intended for fetal applications ("FDA limit").

In addition to the standard output reporting methodology,

measurements were taken to determine the effect, if any, of reflections from the contralateral side of the mouse during scanning. A euthanized 16-week pregnant mouse was shaved on both ventral sides and interposed between the ultrasound transducer and the measurement hydrophone in the same orientation and distance as was done in the exposure experiment. The results indicated that there was little possibility of a reflection adding substantially to the exposure at the fetuses. The final experiment was conducted to measure the actual ultrasound exposure at the fetuses, by inserting a needle hydrophone (Pinducer transducer; Valpey–Fisher, Hopkinton, MA) through an incision on the contralateral side of another anesthetized 16-week pregnant mouse. Multiple measurements were made and averaged; the results can be found in Table 3, which is published as supporting information on the PNAS web site.

Exposure Schedule. At 8 a.m., pregnant mice carrying E16 fetuses received an i.p. injection of BrdU (50 mg/kg) and were then exposed to diagnostic ultrasound in multiple sessions for a total of 5, 15, 30, 60, 210, and 420 min, cumulatively, during the E16–E18 period (Table 1). In the 5- and 15-min experiments, the animals received a single exposure of USW for 5 and 15 min, respectively. This range was meant to approximate that of exposures used in humans. The first ultrasound exposures commenced 12 h after the BrdU injection. In the 30-min experiments, two 15-min exposures were given at 12 and 24 h after the BrdU injection. In the 60-min experiment, two 30-min exposures were given at 12 and 24 h after the BrdU injection. In the 210-min experiment, eight exposures lasting 30 min each were administered. In this case, the first exposure began 8 h after the BrdU injection. In the 420-min experiment, 12 exposures lasting 35 min were given every 4 h. The first exposure also started 8 h after the BrdU injection. In multiple exposure experiments, we changed the side of the exposure with every subsequent treatment.

In addition to the ultrasound-exposed and sham control animals, three additional pregnant dams were injected at E16 with BrdU and placed immediately in the animal care facility without handling until each came to term (three litters with 30 pups total). The P10 offspring were analyzed by using the same methodology as the other two conditions, and these data served as the normal control condition.

Immunohistochemistry and Analysis. The pregnant mice each received a single i.p. injection of 5 mg/ml BrdU dissolved in 0.9% NaCl with 0.007 M NaOH, at a dosage of 50 mg per kilogram of body weight, ≈12 h before beginning the exposures. All pups were euthanized at P10 and perfused with 4% paraformaldehyde. Any experiment in which the control and ultrasound pups were born more than 24 h apart was not included in the analysis. The brains were removed and drop-fixed for 48 h. Three coronal slices from each brain were used for quantification. Sections 100 μm thick were cut on a standard vibratome. The slices were treated with 2 M HCL for 20 min at room temperature, washed three times for 10 min with PBS, and incubated in anti-BrdU at 1:100 (Becton Dickinson, Franklin Lakes, NJ) for 48 h at 4°C and species-specific fluorophore-labeled secondary antibodies at room temperature. The slices were then counterstained with propidium iodide and mounted in Vectashield (Vector Laboratories, Burlingame, CA). Images from a single optical section were taken with a confocal LSM 510 NLO system (Zeiss, Thornwood, NY) with a 25 × 0.8 numerical aperture Plan-NEOFLUAR lens. Images were collected from the medial somatosensory cortex of all animals (Fig. 2). Images were merged into one montage spanning from the pia to the ependymal surface, and $BrdU^+$ cells were counted in PhotoShop 6.0 (Adobe Systems, San Jose, CA). Six montages from each brain were counted. A 10-tiered grid was overlaid on top of the montage, and positively labeled cells were assigned to each tier depending on their placement (Fig. 2). The bottom line of tier 1 started at the top of cortical layer II, and tier 10 ended in the white matter. Each tier was equal in width and height. All imaging and counting were done blind to experimental conditions.

For double-labeling studies, slices were incubated with anti-BrdU at 1:100 (Accurate, Westbury, NY) and anti-NeuN at 1:200 (Chemicon, Billerica, MA), FoxP2 at 1:1,000 (Abcam, Cambridge, MA), or Brn1 at 1:1,300 (Santa Cruz Biotechnology, Santa Cruz, CA) for 48 h at 4°C followed by species-specific, fluorophore-labeled secondary antibodies at room temperature. The slices were then counterstained with ToPro-3 (Molecular Probes, Eugene, OR) and mounted in Vectashield (Vector Laboratories). A stack of five optical slices separated by 2 μm each was taken at images near the ependyma. Counts for the double-labeling of NeuN and BrdU were taken from three montages spanning from pia to ependyma from one control brain and one USW brain exposed for 30 min.

Statistical Analysis. The data were organized for analysis by summing the cell counts for each of the 10 bins across all six slides for each animal (Table 1). The dependent measure, dispersion, was calculated for each animal by computing the percentage of cells found in the lower five bins (bins 6–10). A multiple linear regression model was used to estimate the independent contributions of ultrasound and of treatment duration to dispersion. (Treatment duration may have an independent effect because prolonged handling is stressful for a pregnant animal.) The model predicted dispersion from condition (ultrasound or sham control), duration of treatment, and their interaction. $DISPERS = a + b_1 \cdot COND + b_2 \cdot DUR + b_3 \cdot COND \cdot DUR + \text{error}$ (Table 1).

We are grateful to C.-Y. Kuan, S. Landis, D. Purves, B. Shaywitz, S. Shaywitz, and G. M. Shepherd for advice and comments on the paper. Statistical analysis was performed by Leonid Rozenblit (Prometheus Research, New Haven, CT). This work was supported by the National Institute of Neurological Disorders and Stroke, National Institutes of Health.

1. Mountcastle, V. B. (1997) *Brain* **120,** 701–722.
2. Angevine, J. B., Jr., & Sidman, R. L. (1961) *Nature* **192,** 766–768.
3. Rakic, P. (l974) *Science* **l83,** 425–427.
4. Sidman, R. L. & Rakic, P. (1973) *Brain Res.* **62,** 1–35.
5. Rakic, P. (1972) *J. Comp. Neurol.* **145,** 61–84.
6. Rakic, P. (1988) *Science* **241,** 170–176.
7. Caviness, V. S., Jr., & Rakic, P. (1978) *Annu. Rev. Neurosci.* **l,** 297–326.
8. Barth, P. G. (1987) *J. Neurol. Sci.* **14,** 1–16.
9. Miller, M. W. (1986) *Science* **233,** 1308–1311.
10. Rakic, P. (1988) *Prog. Brain Res.* **73,** 15–37.
11. Gleeson, J. G. & Walsh, C. A. (2000) *Trends Neurosci.* **23,** 352–359.
12. Buxhoeveden, D. P. & Casanova, M. F. (2002) *Brain* **125,** 935–951.
13. Rakic, P. (1990) *Experientia* **46,** 882–891.
14. Kriegstein, A. R. & Noctor, S. C. (2004) *Trends Neurosci.* **27,** 392–399.
15. Marin, O. & Rubenstein, J. L. (2001) *Nat. Rev. Neurosci.* **2,** 780–790.
16. Letinic, K., Zoncu, R. & Rakic, P. (2002) *Nature* **417,** 645–649.
17. Ang, E. S. B. C., Jr., Haydar, T. F., Gluncic, V. & Rakic, P. (2003) *J. Neurosci.* **23,** 5805–5815.
18. Rakic, P., Cameron, R. S. & Komuro, H. (1994) *Curr. Opin. Neurobiol.* **4,** 63–69.
19. Hatten, M. E. & Mason, C. A. (1990) *Experientia* **46,** 907–916.
20. Rivas, R. J. & Hatten, M. B. (1995) *J. Neurosci.* **15,** 981–989.
21. Rakic, P., Knyihar-Csillik, E. & Csillik, B. (1996) *Proc. Natl. Acad. Sci. USA* **93,** 9218–9222.
22. Lidow, M. S. (1995) *Synapse* **21,** 332–341.
23. Kemper, T. L., Lecours, A., Gates, M. J. & Yakovlev, P. I. (1973) *Early Dev.* **51,** 23–62.
24. Schull, W. J., Dobbing, J., Kameyama, Y., O'Rahilly, R., Rakic, P. & Silini, G. (1986) *Ann. ICRP* **16,** 1–43.
25. Algan, O. & Rakic, P. (1997) *J. Comp. Neurol.* **381,** 335–352.
26. Devi, P. U., Suresh, R. & Hande, M. P. (1995) *Radiat. Res.* **141,** 314–317.
27. Tarantal, A. F. & Hendrickx, A. G. (1989) *Teratology* **39,** 149–162.

28. Stark, C. R., Orleans, M., Haverkamp, A. D. & Murphy, J. (1984) *Obstet. Gynecol.* **63,** 194–200.
29. Newnham, J. P., Evans, S. F., Michael, C. A., Stanley, F. J. & Landau, L. I. (1993) *Lancet* **342,** 887–891.
30. Kieler, H., Cnattingius, S., Haglund, B., Palmgren, J. & Axelsson, O. (2001) *Epidemiology* **12,** 618–623.
31. Campbell, J. D., Elford, R. W. & Brant, R. F. (1993) *Can. Med. Assoc. J.* **149,** 1435–1440.
32. Siegel, E., Goddard, J., James, A. E., Jr., & Siegel, E. P. (1979) *Radiology* **133,** 175–179.
33. Liebeskind, D., Bases, R., Koenigsberg, M., Koss, L. & Raventos, C. (1981) *Radiology* **138,** 419–423.
34. Ellisman, M. H., Palmenr, D. E. & Andre, M. P. (1987) *Exp. Neurol.* **98,** 78–91.
35. Stanton, M. T., Ettarh, R., Arango, D., Tonra, M. & Brennan, P. C. (2001) *Life Sci.* **68,** 1471–1475.
36. Fowlkes, J. B. & Holland, C. K. (2000) *J. Ultrasound Med.* **19,** 69–72.
37. Rakic, P. (l971) *J. Comp. Neurol.* **l4l,** 283–3l2.
38. Lewin, P. A. (2004) *Ultrasonics* **42(1),** 367–372.
39. Lewin, P. A. & Bjorno, L. (1982) *J. Acoust. Soc. Am.* **71,** 728–734.
40. Haydar, T. F., Ang, E., Jr., & Rakic, P. (2003) *Proc. Natl. Acad. Sci. USA* **100,** 2890–2895.
41. Blinkov, M. S. & Gleser, I. I. (1968) *The Human Brain in Figures and Tables* (Plenum, New York).
42. Rakic, P. (2003) *Glia* **43,** 19–32.
43. Rakic, P. (2002) *Clin. Neurosci. Res.* **2,** 29–39.
44. Rados, C. (2004) *FDA Consum. Mag.* **38(1),** available at www.fda.gov/fdac/features/2004/104_images.html.
45. Sidman, R. L. & Rakic, P. (1982) in *Histology and Histopathology of the Nervous System*, eds. Haymaker, W. & Adams, R. D. (Thomas, Springfield, IL), pp. 3–145.
46. National Electrical Manufacturers Association (2003) *Acoustic Output Measurement Standard for Diagnostic Ultrasound Equipment*, Standards Publication UD 2-2003 (Natl. Electric. Manuf. Assoc., Rosslyn, VA), Revision 1.
47. National Electrical Manufacturers Association (2003) *Standard for Real-Time Display of Thermal and Mechanical Acoustic Output Indices on Diagnostic Ultrasound Equipment*, Standards Publication UD 3-2003. (Natl. Electric. Manuf. Assoc., Rosslyn, VA), Revision 2.
48. Center for Devices and Radiological Health (1997) *Information for Manufacturers Seeking Marketing Clearance of Diagnostic Ultrasound Systems and Transducers* (Food and Drug Admin., Rockville, MD).
49. Schafer, M. E. & Lewin, P. A. (1988) in *IEEE Trans. Ultrason. Ferroelectrics Freq. Control* **35(2),** 102–109.